Transient Structural Ordering of the RNA-Binding Domain of Carnation Mottle Virus p7 Movement Protein Modulates Nucleic Acid Binding

Marçal Vilar,[a] Ana Saurí,[a] Jose F. Marcos,[b] Ismael Mingarro,*[a] and Enrique Pérez-Payá*[c]

Plant viral movement proteins bind to RNA and participate in the intra- and intercellular movement of the RNAs from plant viruses. However, the role and magnitude of the conformational changes associated with the formation of RNA–protein complexes are not yet defined. Here we describe studies on the relevance of a pre-existing nascent α-helix at the C terminus of the RNA-binding domain of p7, a movement protein from carnation mottle virus, to RNA binding. Synthetic peptide analogues and single amino acid mutation at the RNA-binding domain of recombinant p7 protein were used to correlate the transient structural order in aqueous solution with RNA-binding potential.

Introduction

The interactions in macromolecular assemblies form unique structures that direct/regulate biological functions. These assemblies can generally undergo local macromolecular folding events that are important in the formation of intermolecular complexes. One such complex is that of proteins with RNA, here induced fit takes place in both macromolecules upon binding.[1] In plants, specific RNAs can traffic between cells through plasmodesmata (PD, plant intercellular connections) following the formation of ribonucleoprotein (RNP) complexes with specific proteins.[2] This knowledge was first gained from studies on viral infection.[3,4] In these processes, plant viral MPs actively participate in the intra- and intercellular movement of RNAs from viruses to such an extent that MP dysfunction impairs viral infection.[5,6] Plant viral MP function is probably best illustrated by the fact that several MPs can induce transport of different movement-defective viruses by transcomplementation. This has been exemplified in the case of an insect virus in which cell-to-cell and systemic spread in transgenic plants that express the MP of least two different plant viruses has been reported.[7] In fact, most viral MPs appear to confiscate an endogenous signaling pathway that operates through the regulated intercellular movement of so-called non-cell-autonomous proteins (NCAP).[2] These proteins can be regarded as "viral" NCAP, and are ideal tools for dissecting the functioning of this pathway.[2,8,9]

MP properties are best described in the TMV model system. TMV MP is a multidomain protein that names the "30 K" superfamily of MPs, which comprises proteins from a number of virus groups.[10] TMV MP binds viral ssRNA and ssDNA in vitro with no sequence specificity,[11] colocalizes with the cytoskeleton and cell wall,[12–15] is required for the association of viral RNA with the endoplasmic reticulum,[16] increases the size-exclusion limit (SEL) of PD,[17] and folds as an α-helical membrane protein in the presence of urea and SDS.[18] It has been proposed[4] that TMV MP and viral RNA form a RNP complex[19] that is targeted to (and opens) the PD. The complex is thought to mediate the active transport of the viral genome into the adjacent cell, thus contributing to viral spread. Several plant NCAPs have already been identified. Recently, the first specific component of the plant trafficking apparatus was isolated (NtNCAPP1) and shown to interact and regulate the function of some plant NCAP (e.g., CmPP16) and viral MPs (e.g., TMV MP).[20] CmPP16 was reported to be the first plant paralogue of a viral MP and shares properties with them, such as nonspecific nucleic acid binding, cell-to-cell trafficking of RNA, and increased PD SEL.[21]

Despite their pivotal role and the importance of their interaction with RNA, no plant viral MP structures have yet been solved. This is probably due to the difficulty of obtaining high-resolution structural information for multidomain proteins. Unlike TMV, there are viruses that encode multiple MPs. Furthermore, the MP functions map to separate proteins and act in coordination in the cell-to-cell and long-distance movement of the virus. The type member of Carmovirus group is CarMV

[a] *Dr. M. Vilar,[+] A. Saurí,[+] Dr. I. Mingarro*
Departament de Bioquímica i Biologia Molecular
Universitat de València, 46100 Burjassot (Spain)
Fax: (+34) 963-544-635
E-mail: ismael.mingarro@uv.es

[b] *Dr. J. F. Marcos*
Departamento de Ciencia de los Alimentos
Instituto de Agroquímica y Tecnología de Alimentos–CSIC
Apartado de Correos 73, 46100 Burjassot (Spain)

[c] *Dr. E. Pérez-Payá*
Centro de Investigación Príncipe Felipe and CSIC
Avda. Autopista del Saler 16, 46013 Valencia (Spain)
Fax: (+34) 963-289-701
E-mail: eperez@ochoa.fib.es

[+] *These authors contributed equally to this work.*

 DOI: 10.1002/cbic.200400451

and encodes two such MPs, p7 and p9. We have previously proposed that their small size makes these proteins suitable models for the structural characterization of MPs and their interaction with viral RNA. Following this rationale, CarMV p7 was characterized as a soluble protein with RNA-binding capacity,[22,23] and p9 was characterized as an integral membrane protein.[24] Moreover, p7 was shown to present three distinct protein regions, which include a central RNA-binding domain that contains amino acids 17–35 (p7 sequence numbering, see ref. [23]). Interestingly, a limited sequence homology between CarMV p7 and CmPP16 at the RNA-binding domain has been proposed.[23] A synthetic peptide defining such a domain ($p7_{17-35}$) was structurally characterized and shown to undergo a conformational transition towards the stabilization of an α-helix upon RNA binding. This takes place with a concomitant conformational change in the RNA molecule.[23] Furthermore, NMR analysis of the RNA-free form of $p7_{17-35}$ suggested the presence of a nascent α-helix conformation at the C terminus of the peptide.[23] (In the presence of RNA, the peptide aggregates at the concentration required for NMR analysis.) Although, the importance of this preordered secondary structure for the RNA-binding process was not explored. Nascent secondary-structure elements can also be thought of as transiently ordered states in solution that could facilitate the appropriate interface between a defined protein and its cognate ligand.[25,26] Questions remain, however, regarding the exact nature of the different interfaces that are essential to generate unique structures, in particular in RNA–protein interactions.

In this study, we investigated the relevance of a preexisting nascent α-helix at the C terminus of the p7 RNA-binding domain and studied its correlation with RNA-binding functions. Two synthetic peptide analogues of $p7_{17-35}$, each containing a proline residue that replaces specifically located alanine residues, were used to correlate the transient structural order in aqueous solution with RNA-binding potential. Also, by using single amino acid mutations in p7-recombinant proteins, we showed that such structure–function relationship can also be observed for p7 protein.

Results

In our previous study on the retrostructural characterization of p7, the internal peptide, $p7_{17-35}$, was demonstrated to define the RNA-binding domain of the protein. It was characterized by CD spectroscopy as an α-helical inducible peptide due to its tendency to adopt such a secondary structure in the presence of inducers or viral RNA (Table 1).[23] The NMR characterization of $p7_{17-35}$ in aqueous solution suggested that the C-terminal segment (sequence ^{29}AKDAIRK^{35}) could adopt preordered states in solution, mainly a nascent α-helix. This segment is highly conserved in other MP from carmoviruses[27] and it contains amino acids important for RNA-binding (Ile33, Arg34, and Lys35).[23]

In order to confirm the existence and relevance of the C-terminal nascent α-helix for RNA-binding properties, we designed proline substitution analogues of $p7_{17-35}$. Proline is frequently found at the N terminus but not in the middle of α-helices. It has been suggested that proline has a dual role depending on its position in a helix: either as an initiator at the N-cap or as helix breaker at positions higher than N2 from the N-cap (see values and nomenclature in ref. [28]). Thus, we separately replaced Ala29 and Ala32 by proline (positions N-cap and N3, respectively, in the above-mentioned nascent α-helix) to obtain the synthetic peptides $p7_{17-35}$A29P and $p7_{17-35}$A32P (Table 1). Our rationale for the design of these peptides was as follows: if the preexistence of a nascent helix from amino acid 29 to 35 is important for RNA binding, then the analogue, $p7_{17-35}$A29P, should retain most of the RNA-binding capabilities. However, analogue $p7_{17-35}$A32P should have a diminished affinity for RNA binding because Pro32 will preclude the formation of the nascent helix. In fact, nucleic acid binding, as evaluated by gel shift assay, suggested that peptide $p7_{17-35}$A29P had a RNA binding affinity comparable to that of the parental peptide (Figure 1A and k_D values in Table 1). However, $p7_{17-35}$A32P showed a clear diminished affinity. Table 1 reports its k_D value as >10 μM because peptide solubility at higher concentrations in the presence of RNA precluded more precise determination. Conformational analyses of $p7_{17-35}$A29P and $p7_{17-35}$A32P were conducted by CD spectroscopy and compared with those of the parental peptide. In aqueous solution, all three peptides are highly flexible without discernible secondary structure (data not shown). However, propensity to fold into an α-helix in the presence of 5 mM SDS and 50% TFE (not shown) relates with the RNA-binding activity of the peptides (Figure 1B and Table 1).

Table 1. Names, sequences, and properties of the CarMV p7-derived synthetic peptides used in this study.

Name	Sequence	k_D [μM][a]	α-helix (%)[b] SDS/TFE
$p7_{17-35}$	Ac-GNRGKQKTRRSVAKDAIRK-NH_2	3.4 ± 1.2	60:40
$p7_{17-35}$A29P	Ac-GNRGKQKTRRSV**P**KDAIRK-NH_2	4.7 ± 0.7	27:21
$p7_{17-35}$A32P	Ac-GNRGKQKTRRSVAKD**P**IRK-NH_2	>10	16:14

[a] Apparent dissociation constant (k_D) of RNA-binding defined as in ref. [23] [b] The percentage of α-helix content was calculated from the CD spectra of the peptides in the presence of 5 mM SDS or 50% (*v/v*) TFE (see Experimental Section).

The peptides were also analyzed by NMR spectroscopy in two solvents: H_20 and 50% TFE. Peptide concentrations of 2.6 mM were used in the NMR studies and sequence-specific assignments were made by using a combination of TOCSY, phase sensitive double quantum filtered COSY, and ROESY methods. The adoption of a defined preferential secondary structure by a peptide induces significant and specific chemical shift changes in ^{1}H nuclei that can be used to quantify secondary-structure populations. In particular, an α-helical conformation in peptides and proteins is characterized by upfield shifts of the αH.[29,30] Figure 2 summarizes the conformational shifts (i.e., the deviation of the chemical shifts for each residue from those attributed to random coil values)[31,32] for peptides $p7_{17-35}$, $p7_{17-35}$A29P, and $p7_{17-35}$A32P. The data for $p7_{17-35}$ and $p7_{17-35}$A29P in aqueous solution and in 50% TFE further confirm the presence of a nascent α-helical conformation at the C

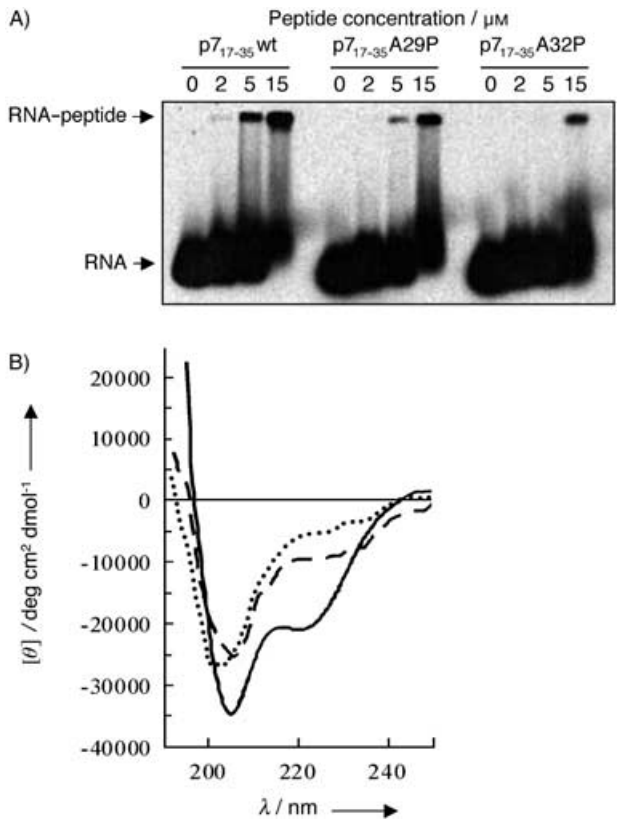

Figure 1. RNA-binding and secondary-structure characterization of synthetic peptide analogues derived from CarMV p7 RNA-binding domain. A) EMSA for RNA binding of peptides p7$_{17-35}$, p7$_{17-35}$A29P, and p7$_{17-35}$A32P. Increasing concentrations of peptides were incubated with ssRNA probe (see Experimental Section). B) Far-UV CD spectra of peptides p7$_{17-35}$wt (——), p7$_{17-35}$A29P (-----), and p7$_{17-35}$A32P (····) in the presence of SDS (5 mM). Peptide concentration was 20 μM in MOPS/NaOH buffer (5 mM, pH 7.0) at 25 °C.

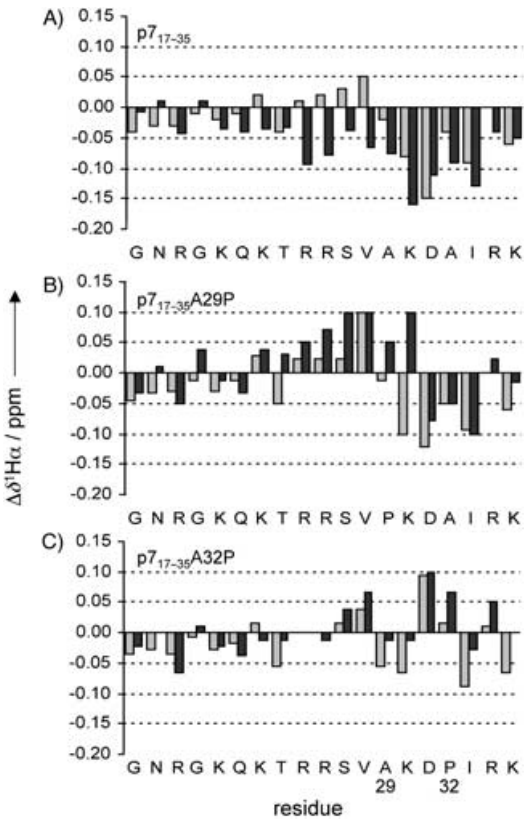

Figure 2. NMR analysis of peptides A) p7$_{17-35}$ (data from ref. [23] with permission from the American Society for Biochemistry and Molecular Biology), B) p7$_{17-35}$A29P, and C) p7$_{17-35}$A32P in water (gray bars) and in the presence of 50% TFE (black bars). Observed conformational chemical shift increments for ^{1}H ($\Delta\delta^1$Hα) relative to the chemical shifts of random-coil values.

terminus of the peptides from Pro29 to Lys35. As expected, the NMR analysis of p7$_{17-35}$A32P showed that the C terminus of this peptide adopts a random conformation (Figure 2). It should be noted that, in the presence of TFE, the amino acid sequence of peptide p7$_{17-35}$ allows the propagation of the α-helical conformation from the C to the N terminus up to residue Arg25. However, the presence of proline in p7$_{17-35}$A29P precludes such a helical propagation and circumscribes the helical conformation at the C-terminal segment. This is apparent from the conformational shift deviation diagrams, in which residues preceding the prolines always exhibit strong positive deviations from random-coil values; this is indicative of extended conformations. Interestingly, a similar pattern of conformational extension has recently been found in peptides that harbor proline replacements. This has further demonstrated the relevance of a helical region in molecular recognition events.[33]

To further corroborate the importance and relevance of the C-terminal nascent α-helix in RNA-binding properties, we prepared mutant p7 proteins with the same point mutations that were found to be relevant with synthetic peptides. All three recombinant proteins, p7wt (p7 wild-type), p7A29P, and p7A32P, were purified from inclusion bodies and subjected to a refold-

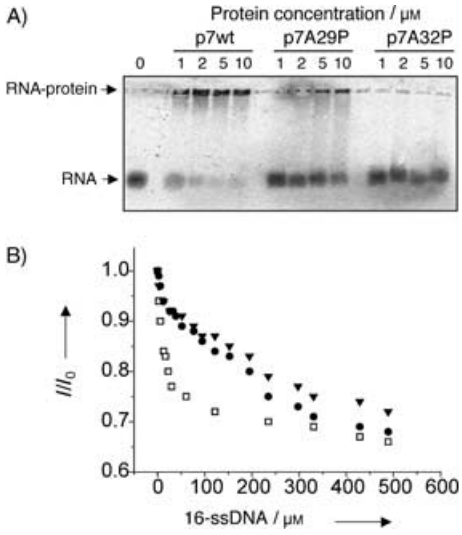

Figure 3. Nucleic acid binding capacity of recombinant p7 derived protein mutants. A) EMSA for RNA binding of p7wt, p7A29P, and p7A32P. Increasing concentrations of refolded proteins (up to 10 μM) were incubated with ^{33}P-labeled ssRNA probe (see Experimental Section). B) Trp fluorescence quenching experiments of p7-derived proteins with 16-ssDNA. Protein–nucleic acid association was estimated from Trp fluorescence changes in the presence of increasing concentrations of 16-ssDNA (*x* axis). (□) p7wt; (●) p7A29P; (▼) p7A32P. Protein concentration in all cases was 5 μM.

ing procedure (see Experimental Section). Figure 3 shows representative EMSA analysis of viral RNA binding to recombinant p7wt, p7A29P, and p7A32P. Increased concentrations of p7wt lowered the amount of free RNA and resulted in the formation of high-molecular-weight RNA–p7 complexes that were detectable with 1 μM of total protein (Figure 3A). The amount of RNA–protein complex formation was lower with p7A29P and p7A32P than that obtained with p7wt (Figure 3A). However, while protein p7A29P retained, in part, the RNA-binding activity (as suggested by the formation of large RNA–protein complexes), this property was almost totally impaired in protein p7A32P. The absence of detectable intermediate complexes in EMSA (a common feature in the RNA-binding properties of MPs) suggested an "all-or-none" mechanism that can be attributed to a highly cooperative binding process and that poses difficulties for quantitative analysis. Furthermore, when we titrated a solution of p7wt protein with viral RNA and followed the changes in fluorescence emission of the unique Trp59 of p7, we observed an increase in the turbidity of the solution, which hindered quantitative spectroscopic analyses. This suggested the formation of insoluble high-molecular-weight RNA–protein complexes. Most of the MPs that bind to ssRNA also have ssDNA-binding properties.[22,34–36] Thus, in an attempt to bypass the problems of RNA–protein aggregation and to obtain a more accurate quantitative description of the binding process,[37] we used short ssDNA of different lengths. In this way we avoided the multiple binding of proteins to a single nucleic acid molecule that was probably the cause of the observed complex insolubility. We used two unrelated ssDNA oligonucleotides of 16 (16-ssDNA) and 27 nucleotides (27-ssDNA) in length and analyzed their binding to p7wt with EMSA. 27-ssDNA showed a binding profile similar to that obtained for RNA ("all-or-none" mechanism). The 16-ssDNA–p7 complex was only partially retarded in the gel and did not form high-molecular-weight aggregates that could interfere in a quantitative binding assay by fluorescence spectroscopy (results not shown). Figure 3B shows the decrease in the intrinsic fluorescence of Trp59 when solutions of p7wt, p7A29P, and p7A32P were titrated with a concentrated stock solution of 16-ssDNA. The fluorescence-spectroscopy data analysis allowed the estimation of the relative dissociation equilibrium constants for the ssDNA–protein complexes; these were 12 ± 1, 169 ± 17, and 185 ± 22 μM for p7wt, p7A29P, and p7A32P, respectively.

Discussion

The high-resolution structure of plant viral MPs in the presence or absence of the cognate RNA is still missing because of difficulties in obtaining protein or RNA–protein complexes that are suitable for structural analysis. To circumvent these limitations, we have adopted a protein dissection approach to gain information on the structural and RNA-binding properties of this class of proteins.[23,24] This has allowed, among other features, the identification of the RNA-binding domain of the CarMV p7 movement protein. In this study, we have examined the functional role of a nascent α-helix that was previously identified at the C terminus of the RNA-binding domain.[23]

Our data suggest that $p7_{17–35}$ defines the RNA-binding domain of p7 and adopts a nascent helical structure in solution that implies the involvement of the segment ^{29}AKDAIRK^{35}. This segment is almost absolutely conserved in different isolates of CarMV and highly conserved in other carmo- or necroviruses.[22,27] The helix is further stabilized by charge neutralization in the presence of negatively charged templates, such as the secondary structure inducer SDS at submicellar concentrations (Figure 1B), and RNA or TFE.[23] Replacement of Ala29 by Pro at the N-cap of the helix (peptide $p7_{17–35}$A29P) did not significantly alter the folding of the native peptide in aqueous solution as deduced from the NMR experiments. However, this replacement reduced the propensity to fold in the presence of secondary structure inducers. This restricted the α-helical structure to the segment spanning Pro29 to the C terminus, instead of the previously observed propagation of the nascent helix to the N terminus in $p7_{17–35}$ (Figure 2A vs. B). This residue replacement has a minor, but consistent, contribution in decreasing the RNA-binding capability of the peptide (Figure 1A). Replacement of Ala32 with Pro ($p7_{17–35}$A32P) precluded the adoption of the α-helical structure at the C terminus of the domain and had a major effect on RNA-binding affinity (peptide $p7_{17–35}$A32P has a lowered binding affinity to viral RNA compared with $p7_{17–35}$A29P and $p7_{17–35}$). The higher efficiency in RNA binding of the native sequence, comparable to that of the proline-mutated peptides, thus seems to be governed by the C-terminal conformation of the RNA-binding domain. This could play an important role in promoting RNA–full-length MP recognition.

The information obtained on RNA-binding requirements by using synthetic peptides can, at least in part, be useful in understanding more complex systems, that is, the full-length protein. The protein p7A32P has lower affinity than the less severe mutant p7A29P in binding nucleic acids (Figure 3). Thus, point mutations that do not change the net charge of the protein diminish nucleic acid binding, most likely through a conformational alteration of the RNA-binding domain. Such alterations could be critical for the in vivo functions of the viral protein.

In conclusion, the results suggest that not only modules but also nascent secondary-structure units that can be stabilized early in the protein-folding pathway could have functional and structure-forming capabilities. It is feasible to postulate that, as demonstrated for the synthetic RNA-binding domain and for the full-length p7 protein, the stabilization of a nascent α-helical conformation at the C terminus of the RNA-binding domain is important for the molecular mechanism associated with the interaction between viral RNA and CarMV MP. Such a nascent structure could reduce the amount of free energy that is required for the transition ("unordered to helix") observed upon binding to nucleic acid. A similar observation has been recently reported on the role of helix-capping residues in peptides that are derived from DNA-binding proteins.[38]

The rate of formation of intramolecular interactions in unfolded proteins determines how fast conformational space can be explored during folding and it is essential for the understanding of the earliest steps in protein folding. This principle could be of wider application and could also apply to intermo-

lecular RNA–protein interactions. The presence of nascent secondary structure elements does not diminish the structural freedom that these crucial proteins probably need for their function. However, they decrease the conformational space that needs to be explored for the formation of productive RNA–protein interactions.

Experimental Section

Materials: *N*-Fmoc protected amino acids for peptide synthesis were from SENN Chemicals (Dielsdorf, Switzerland). Site-directed mutagenesis was performed by using the QuikChange kit from Stratagene. RNA in vitro transcription kit was from Promega, and digoxigenin (DIG) detection kit was from Roche. Deuterium oxide (^2H_2O) and [D_3]TFE were from Cambridge Isotopes Labs (Andover, USA). [α-^{33}P]UTP was from Hartmann Analytic (Braunschweig, Germany). All other chemicals were from standard suppliers.

Peptide synthesis: Peptides were synthesized as acetylated N- and C-terminal amides by using standard Fmoc chemistry on a 433 A peptide synthesizer (Applied Biosystems) and purified by RP-HPLC. Matrix-assisted laser desorption ionization-time-of-flight mass spectrometry was use to confirm peptide identity. Peptide concentrations were determined by quantitative amino acid analysis for RNA-binding assays and spectroscopy studies.

CD spectroscopy: All measurements were carried out on a Jasco J-810 CD spectropolarimeter in conjunction with a Neslab RTE 110 waterbath and temperature controller. CD spectra were the average of a series of ten scans made at 0.2 nm intervals. CD spectra of the solution buffer without peptide (or in the presence of SDS as described in the figure legends) were used as baseline in all the experiments. The helical content was evaluated based on a theoretical value of 100% helix as calculated by $FH = FH^8(1-k/n)$, where FH^8 is $-40000°cm^2dmol^{-1}$;[39] the wavelength-dependent constant, k, is 2.5; and n is the number of residues. The theoretical $[\theta]_{222}$ value for 100% α-helix for a 19-residue peptide is $-34736°cm^2dmol^{-1}$.

NMR spectroscopy: Peptide samples (2.6 mM) were prepared in two solvents: water and TFE/water (1:1, *v/v*). NMR spectra were acquired at 283 K on a Bruker Avance spectrometer that operated at 500 MHz, and data were analyzed as reported.[23]

Heterologous production, purification, and refolding of p7wt, p7A29P, and p7A32P: p7 proteins were produced and purified as previously described.[23] A refolding protocol was carried out with the purified protein in buffer A (6 M guanidinium-HCl, 20 mM sodium phosphate, 2 M urea, 0.3 M NaCl, 10% sucrose, 0.5 M arginine, 50 mM glycine, 2 mM EDTA, and 0.01 M NaOH, pH 5.5). The solution was dialyzed successively against decreasing concentrations of guanidinium-HCl (4, 2, 1, and 0 M) in the same buffer.

EMSA experiments: Different amounts of synthetic peptides were incubated with the 181 ribonucleotide residue pCarM.D5 ssRNA probe (1 ng)[22] in binding buffer (final volume 10 μL; 10 mM Tris-HCl, pH 8.0, 1 mM EDTA, 100 mM NaCl, 5 units HRPI RNase inhibitor (Promega), 10% glycerol) for 30 min on ice.[23] After incubation, loading buffer was added (2 μL), and the samples were electrophoresed through an agarose (1%) in TAE buffer (40 mM Tris-acetate, 2 mM EDTA) at 50 V for 40 min at 4°C. RNA was transferred to positively charged nylon membranes by capillary elution in 20xSSC (3 M NaCl, 0.3 M sodium citrate·2H_2O) and fixed to the membranes by UV irradiation in a UV gene linker for 2 min. Membranes were hybridized to a digoxigenin-labeled DNA probe in PSE (7% SDS, 1 mM EDTA, 0.3 M sodium phosphate, pH 7.2) at 60°C, overnight. Detection of digoxigenin-labeled nucleic acids was carried out and the amount of free RNA probe was quantified in each sample by densitometry of the films (Quantity One software, Bio-Rad). The apparent dissociation constant (k_D) of the RNA–peptide complex was then determined, as described previously.[23] For EMSA assays with p7wt and mutant proteins, pCarM.D5 ssRNA probe was ^{33}P-labeled by using in vitro T7-polymerase transcription system (Promega). Template DNA was digested with RNase-free DNase after transcription, by following the manufacturer's instructions. Different amounts of protein were incubated with ^{33}P-labelled RNA (0.2 $\mu Ci\,\mu L^{-1}$) in binding buffer (10 μL) and electrophoresed as described. The gels were dried by capillarity and scanned with a Fuji FLA-3000 PhosphorImager by using the Image Reader 1.0 software.

Fluorescence measurements: Fluorescence measurements were carried out at 20°C on a Perkin–Elmer LS-50B spectrofluorimeter by using slit widths within 1 and 5 nm for excitation and emission, depending on each particular experiment. Fluorescence emission spectra of the proteins in MOPS-NaOH (5 mM, pH 7.0) were monitored from 300 to 500 nm and obtained by excitation at 280 nm in a 1 cm quartz cell. Titrations were performed by addition of small aliquots of unspecific 16-ssDNA from a stock solution to the proteins at the desired concentration (final volume 1 mL). The data shown are representative of several independent experiments. Fluorescence contribution from the buffer and/or ssDNA solutions without protein, were used as baseline and subtracted from all experiments.

Abbreviations

- CarMV: carnation mottle virus
- EDTA: ethylenediamine tetraacetic acid
- EMSA: electrophoretic mobility shift assay
- Fmoc: *N*-(9-fluorenyl)methoxycarbonyl
- MOPS: 4-morpholinepropanesulfonic acid
- MP: movement protein
- SDS: sodium dodecyl sulfate
- ssDNA: single-stranded DNA
- ssRNA: single-stranded RNA
- TFE: trifluoroethanol
- TMV: tobacco mosaic virus.

Acknowledgements

This work was supported by grants SAF01-2811 (MCyT), UV-AE-20030395 (Universitat de València), CTIAE/E/03/61 and GV04B-183 (Generalitat Valenciana), Fundación Valenciana de Investigaciones Biomédicas and Spanish MEC (FPU predoctoral fellowship to A.S.). We thank Dr. Vicent Esteve for his advice in the NMR experiments and Alicia García and Ana Giménez for excellent technical work.

Keywords: helical structures · movement protein · NMR spectroscopy · peptides · RNA recognition

[1] J. R. Williamson, *Nat. Struct. Biol.* **2000**, *7*, 834.
[2] W. J. Lucas, J. Y. Lee, *Nat. Rev. Mol. Cell Biol.* **2004**, *5*, 712.

[3] S. G. Lazarowitz, R. N. Beachy, *Plant Cell* **1999**, *11*, 535.
[4] V. Citovsky, P. Zambryski, *Bioessays* **1991**, *13*, 373.
[5] C. M. Deom, M. Lapidot, R. N. Beachy, *Cell* **1992**, *69*, 221.
[6] B. G. McLean, E. Waigmann, V. Citovsky, P. Zambryski, *Trends Microbiol.* **1993**, *1*, 105.
[7] R. Dasgupta, B. H. Garcia, 2nd, R. M. Goodman, *Proc. Natl. Acad. Sci. USA* **2001**, *98*, 4910.
[8] X. L. Wu, D. Weigel, P. A. Wigge, *Genes Dev.* **2002**, *16*, 151.
[9] V. Haywood, F. Kragler, W. J. Lucas, *Plant Cell* **2002**, *14*, S303.
[10] U. Melcher, *J. Gen. Virol.* **2000**, *81*, 257.
[11] V. Citovsky, D. Knorr, G. Schuster, P. Zambryski, *Cell* **1990**, *60*, 637.
[12] C. M. Deom, K. R. Schubert, S. Wolf, C. A. Holt, W. J. Lucas, R. N. Beachy, *Proc. Natl. Acad. Sci. USA* **1990**, *87*, 3284.
[13] M. Heinlein, B. L. Epel, H. S. Padgett, R. N. Beachy, *Science* **1995**, *270*, 1983.
[14] B. G. McLean, J. Zupan, P. C. Zambryski, *Plant Cell* **1995**, *7*, 2101.
[15] E. Waigmann, P. Zambryski, *Plant Cell* **1995**, *7*, 2069.
[16] P. Mas, R. N. Beachy, *J. Cell Biol.* **1999**, *147*, 945.
[17] S. Wolf, C. M. Deom, R. N. Beachy, W. J. Lucas, *Science* **1989**, *246*, 377.
[18] L. M. Brill, R. S. Nunn, T. W. Kahn, M. Yeager, R. N. Beachy, *Proc. Natl. Acad. Sci. USA* **2000**, *97*, 7112.
[19] O. I. Kiselyova, I. V. Yaminsky, E. M. Karger, O. Y. Frolova, Y. L. Dorokhov, J. G. Atabekov, *J. Gen. Virol.* **2001**, *82*, 1503.
[20] J. Y. Lee, B. C. Yoo, M. R. Rojas, N. Gomez-Ospina, L. A. Staehelin, W. J. Lucas, *Science* **2003**, *299*, 392.
[21] B. Xoconostle-Cazares, Y. Xiang, R. Ruiz-Medrano, H. L. Wang, J. Monzer, B. C. Yoo, K. C. McFarland, V. R. Franceschi, W. J. Lucas, *Science* **1999**, *283*, 94.
[22] J. F. Marcos, M. Vilar, E. Pérez-Payá, V. Pallas, *Virology* **1999**, *255*, 354.
[23] M. Vilar, V. Esteve, V. Pallas, J. F. Marcos, E. Pérez-Payá, *J. Biol. Chem.* **2001**, *276*, 18122.
[24] M. Vilar, A. Sauri, M. Monne, J. F. Marcos, G. von Heijne, E. Pérez-Payá, I. Mingarro, *J. Biol. Chem.* **2002**, *277*, 23447.
[25] H. Lee, K. H. Mok, R. Muhandiram, K. H. Park, J. E. Suk, D. H. Kim, J. Chang, Y. C. Sung, K. Y. Choi, K. H. Han, *J. Biol. Chem.* **2000**, *275*, 29426.
[26] E. W. Sayers, R. B. Gerstner, D. E. Draper, D. A. Torchia, *Biochemistry* **2000**, *39*, 13602.
[27] M. C. Canizares, J. F. Marcos, V. Pallas, *Arch. Virol.* **2001**, *146*, 2039.
[28] R. Aurora, G. D. Rose, *Protein Sci.* **1998**, *7*, 21.
[29] K. J. Barnham, T. R. Dyke, W. R. Kem, R. S. Norton, *J. Mol. Biol.* **1997**, *268*, 886.
[30] A. Pintar, A. Chollet, C. Bradshaw, A. Chaffotte, C. Cadieux, M. J. Rooman, K. Hallenga, J. Knowles, M. Goldberg, S. J. Wodak, *Biochemistry* **1994**, *33*, 11158.
[31] D. S. Wishart, B. D. Sykes, *Methods Enzymol.* **1994**, *239*, 363.
[32] K. Wüthrich, *NMR of Proteins and Nucleic Acids*, Wiley, New York, **1986**.
[33] L. Falcigno, R. Oliva, G. D'Auria, M. Maletta, M. Dettin, A. Pasquato, C. Di Bello, L. Paolillo, *ChemBioChem* **2004**, *5*, 1653.
[34] V. Citovsky, M. L. Wong, A. L. Shaw, B. V. Prasad, P. Zambryski, *Plant Cell* **1992**, *4*, 397.
[35] T. A. Osman, R. J. Hayes, K. W. Buck, *J. Gen. Virol.* **1992**, *73*, 223.
[36] F. Schoumacher, M. J. Gagey, M. Maira, C. Stussi-Garaud, T. Godefroy-Colburn, *FEBS Lett.* **1992**, *308*, 231.
[37] A. I. Dragan, J. Klass, C. Read, M. E. Churchill, C. Crane-Robinson, P. L. Privalov, *J. Mol. Biol.* **2003**, *331*, 795.
[38] J. J. Hollenbeck, D. L. McClain, M. G. Oakley, D. G. Gurnon, G. C. Fazio, J. J. Carlson, Y. Lee, *Protein Sci.* **2002**, *11*, 2740.
[39] C. Rohl, A. Chakrabartty, R. Baldwin, *Protein Sci.* **1996**, *5*, 2623.

Received: December 17, 2004
Published online on July 8, 2005

